Surface Segregation and Backscattering in Doped Silicon Nanowires

M. V. Fernández-Serra, Ch. Adessi, and X. Blase

Laboratoire de Physique de la Matière Condensée et Nanostructures (LPMCN), UMR CNRS 5586, Université Claude Bernard Lyon 1, Bâtiment Brillouin, 43 Bd 11 Novembre 1918, 69622 Villeurbanne, France

(Received 13 December 2005; published 27 April 2006)

By means of *ab initio* simulations, we investigate the structural, electronic, and transport properties of boron and phosphorus doped silicon nanowires. We find that impurities always segregate at the surface of unpassivated wires, reducing dramatically the conductance of the surface states. Upon passivation, we show that for wires as large as a few nanometers in diameter, a large proportion of dopants will be trapped and electrically neutralized at surface dangling bond defects, significantly reducing the density of carriers. Important differences between *p*- and *n*-type doping are observed. Our results rationalize several experimental observations.

DOI: 10.1103/PhysRevLett.96.166805 PACS numbers: 73.22.−f, 71.15.Mb, 73.63.−b

The synthesis of semiconducting nanowires has recently renewed the interest that the discovery of carbon nanotubes (CNTs) generated. Because of their compatibility with silicon based technology, silicon nanowires (SiNWs) are being extensively studied and numerous experiments have already characterized some of their structural [1–3] and electronic [4–6] properties. Currently synthesized SiNWs, used in devices such as field effect transistors [7] (FET), are passivated by an oxide layer or by hydrogen [8] and their conduction properties are modified by the type and concentration of the dopants [4,9,10].

Concerning the theoretical aspects, the large fundamental interest related to wire-specific bulk or surface reconstructions explains why most studies to date have focused on the properties of undoped and unpassivated wires [11–16]. Important surface [13] and core [14] reconstructions have been observed, leading to novel properties such as an intrinsic metallic or semimetallic character mediated by dispersive surface states [13,17].

However, one of the main advantages of the use of SiNWs in nanodevices, as opposed to CNTs, stems from their intrinsic semiconducting character which allows conductance to be controlled by doping and application of a gate voltage [4,6,10] in standard FETs. In contrast with CNTs, impurity atoms in SiNWs can be located either in the core or at the surface, highlighting the need to study dopant localization and its related electronic properties. Recent experimental results suggest the segregation of B atoms at the surface of SiNWs [9,18,19].

In addition, due to the large surface to bulk aspect ratio, the question of impurity trapping by surface defects at, e.g., the Si/SiO_2 interface becomes crucial in SiNWs. Taking as a lower bound a concentration of $\sim 10^{12}$ cm^{-2} for interface dangling bond (DB) defects [20,21], one can straightforwardly conclude that with ''bulk'' impurity concentrations of 10^{18}–10^{19} cm^{-3} [22], there are as many surface traps as dopants in SiNWs up to a few nms in diameter. Wires in this size range, starting to compete with multiwall CNTs, are currently synthesized [8] and simulations [23] show that they would be optimal for integration in devices with sub-100 Å gate length.

In this Letter, we analyze the problem of boron and phosphorus segregation in unpassivated and hydrogen-passivated SiNWs by means of *ab initio* simulations. We conclude that impurities always segregate at the surface of unpassivated wires, with segregation energies depending on the impurity type and the surface properties. On the basis of a recently developed O(N) *ab initio* transport approach, we show that such segregation dramatically affects the conductance of surface channels. In the case of passivated surfaces, we find that impurities are trapped and electrically neutralized by surface defects, significantly reducing the carrier concentrations at room temperature for wires up to several nms in diameter. As a result, and as compared to bulk, larger impurity concentrations will be required for equivalent conductivities and a *n*- versus *p*-type resistivity inversion is expected to occur. These two conclusions allow us to rationalize several recent experimental observations [4,6,10].

Methodology.—We perform density-functional theory (DFT) calculations within a generalized gradient approximation to the exchange and correlation functional [24]. Pseudopotentials [25] and a basis set of strictly localized numerical orbitals, are used [26]. Structural relaxations and conductance calculations are performed with a single-ζ polarized basis, increased to double-ζ polarized sets for total energy and band structure calculations. A 4*k*-point grid is used for the reciprocal space sampling along the nanowire axis direction.

Unpassivated wires.—We first study the segregation of B and P in various unpassivated wires displaying different surface reconstructions and electronic properties. Three different systems are considered. Nanowires labeled *a* and *b*, grown along the ⟨100⟩ direction, are described by Rurali *et al.* in Ref. [13]. SiNW-*a* is metallic without doping, due to its particular surface reconstruction, while SiNW-*b* is semimetallic due to a different surface reconstruction associated with a doubling of the SiNW-*a* unit

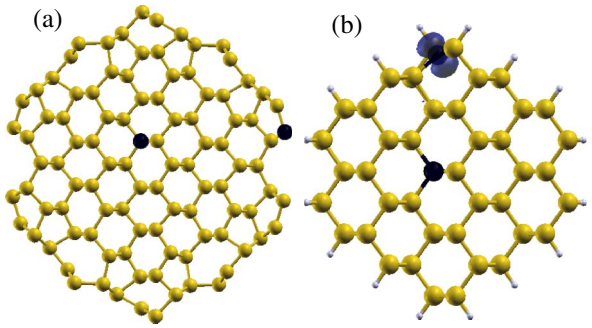

FIG. 1 (color online). ⟨110⟩-grown wires. (a) Unpassivated, surface reconstructed SiNW-*c*, (in black, the bulk and most stable surface dopant positions). (b) *H*-passivated SiNW-*d*, with a density isosurface corresponding to the "B + DB" complex deep into the gap (see text).

cell. An additional system (SiNW-*c*), grown along the ⟨110⟩ direction with (100) and (111) reconstructed facets at the surface [27], is studied (Fig. 1). This last wire has a radius of 15 Å (instead of 8 Å for SiNW-*a* and -*b*) and is metallic with two bands crossing the Fermi level near the *X* point. In order to minimize impurity interactions upon "periodic" doping, the cells of SiNW-*a* and SiNW-*c* are doubled, yielding, respectively, 114 atoms and 200 atoms systems. In the case of SiNW-*a*, we have verified that using a triple cell does not change by more than 10% the energies provided below.

Planar semiconducting Si surfaces have already been studied [29,30]. In agreement with previous work [30], we find a clear tendency for surface segregation in the case, e.g., of a Si(001)-2 × 1 surface (Table I). While large unpassivated SiNWs will certainly yield similar results, the modifications of the structural and electronic surface properties in small wires [13,17] are expected to strongly affect the magnitude, and possibly the sign, of these segregation energies. Further, elastic relaxation effects, previously invoked in the case of planar surfaces [30], may be significantly affected in the limit of small radii.

We report in Table I the surface to bulk energy difference for the most stable surface positions in wires (*a*) to (*c*) [31]. Clearly, even in this limit of small metallic or semimetallic wires, impurities will segregate at the surface, even though the effect is reduced as compared to planar surfaces. Comparing SiNW-*a* to SiNW-*b*, the effect is more pronounced with reduced surface metallicity, consistent with the larger value obtained for semiconducting planar surfaces. These results seem to point to a strong electronic contribution to the surface stabilization.

TABLE I. Segregation energies (in eV, see text). The energy reference is the bulk value.

	Si(001)-2 × 1	Wire *a*	Wire *b*	Wire *c*	Wire *d*
B_{doped}	−0.7	−0.03	−0.14	−0.11	−0.99
P_{doped}	−1.08	−0.98	−1.05	−1.10	−1.62

While one cannot study all possible surface topologies as a function of SiNW diameter and growth direction, our results strongly suggest that in all situations, from small to large diameters, both in metallic and semiconducting wires, impurities will segregate at the surface. As shown below, such a surface segregation will strongly affect the conductance associated with surface states. Further, our results clearly indicate that in all cases, P surface segregation will be more pronounced than B segregation. Therefore, different behavior might be expected upon *n*- or *p*-type doping of SiNWs. We will address this point in more detail after studying the case of passivated wires.

Passivated wires.—Consistent with the conclusion that surface segregation is mainly driven by electronic effects, in the case of fully H-passivated wires and flat surfaces, we do not see any sizeable energy difference between different positions below the surface. However, as emphasized above, the large surface to bulk aspect ratio significantly accentuates the importance of surface or interface defects (Pb-related) which are known to exist at Si/SiO_2 interfaces [20,21]. All of these defects produce a less-coordinated Si surface atom left with at least one DB. To mimic this situation, we generate a 5.6 Å radius H-passivated wire (SiNW-*d* in Fig. 1) grown along the ⟨110⟩ direction [32]. All surface atoms but one are saturated with hydrogen. Two unit cells (124 atoms) are used for this segregation study.

Again, we find (Table I) that impurities prefer to segregate at the surface to passivate DB defects [35]. The segregation energy is found to be much larger than in the case of unpassivated surfaces, indicating again the importance of electronic effects. To further understand the effect of such a segregation, we show in Fig. 2 the band structures for the surface and bulk doped SiNW-*d*. For B in a core position, the wire exhibits a degenerate semiconducting behavior [36] and the unpassivated DB yields an empty (hardly dispersive) band close to the top of the valence bands. However, upon segregation of B at the surface DB site, the "boron + DB" complex yields an empty level deep into the band gap [Fig. 2(b)] with a clear boron p_z

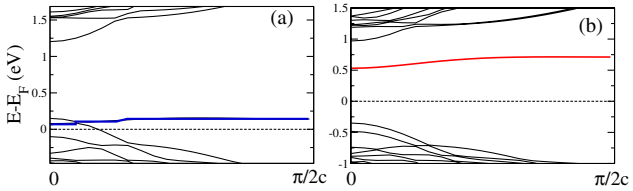

FIG. 2 (color online). Band structure of B doped SiNW-*d*. (a) B in the center of the wire, the system has a degenerate semiconductor character. The blue line represents the DB state. (b) B at the surface, the structure becomes semiconducting, with an isolated B state deep into the gap (red). (Dashed lines indicate the Fermi level)

character, B adopting a planar sp^2-like configuration [Fig. 1(b)]. As a result, the Fermi level rises above the top of the valence bands and the wire becomes truly semiconducting (undoped). The impurity trapped at the surface is electronically inactive and does not yield a carrier at room temperature, as the in-gap level is several thousand K away from the band edges.

The segregation energy of P atoms at the surface is, again, significantly larger than that of B. This means that for the same impurity concentration, a much larger fraction of P atoms will be trapped at the surface and electronically inactive. Namely, the concentration of free carriers will be much larger in the case of B doping than P doping for the same impurity density. Cui *et al.* [4] and Yu *et al.* [6] have reported experimental measurements of conductance in B- and P-doped wires. It is observed that for similar doping levels, B doped SiNWs present a lower resistance than P-doped ones. In bulk doped Si, for the same concentration of these dopants, the effect is known to be exactly the opposite [22].

In both p- and n-type doping, these results suggest that in SiNWs, surface traps can neutralize a significant fraction of impurities up to a critical concentration c_0 that will depend on the wire radius. Below c_0, the conductivity in wires should increase very slowly with doping percentage and p doping should be more efficient than n type (contrary to bulk). Beyond c_0, most impurities will start again to be ionized at room temperature and the relation between impurity and free carrier concentrations will follow that of bulk but with a c_0 shift. As a result, larger dopant concentrations will be necessary in SiNWs as compared to bulk for the same conductivity. This is consistent with the values of resistivity measured in B doped SiNWs which are found to be higher than expected in bulk Si at similar dopant concentrations [10].

Transport.—Beyond information related to the density of free carriers, device performances are also strongly related to the mobility (or mean-free path) of these carriers. In the diffusive regime, such quantities are governed, in particular, by the elastic scattering of electrons by defects (inelastic scattering by phonons will not be addressed). We focus here on the conductance associated with the surface channels of a flat Si(001)-$p(2 \times 2)$ ''alternated dimer'' surface [37] doped by isolated B or P impurities.

Our calculations are based on a recently developed [38] *ab initio* implementation of the Landauer formalism. We start with a ground-state calculation of the system of interest (device and surrounding electrodes) using the SIESTA package. The strictly localized nature of the basis allows to partition the system into nonoverlapping blocks [see Fig. 3(a)] so that the Hamiltonian H and overlap S matrices of the infinite system (device + leads) are tridiagonal by blocks. This property allows the recursive calculation of the Green's function and associated self-energy Σ_L and Σ_R of the left and right semi-infinite electrodes.

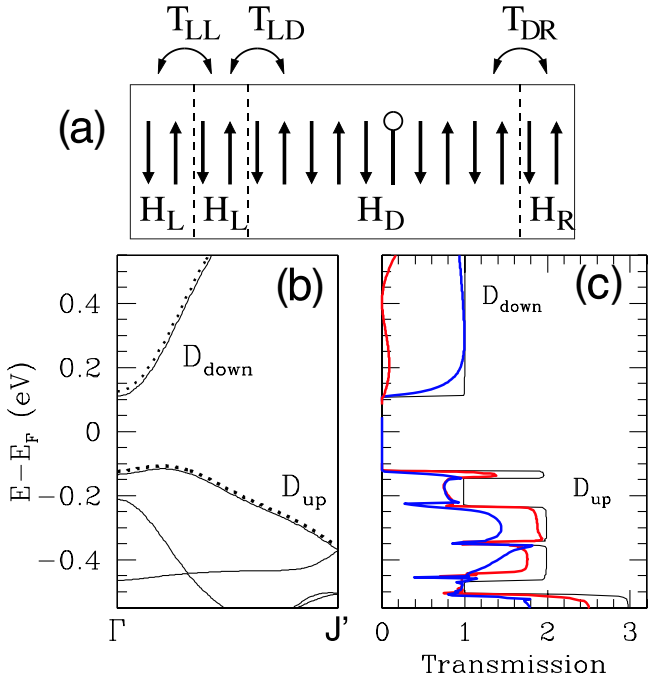

FIG. 3 (color online). (a) Symbolic representation of the partitioning of the supercell in left/right electrodes and central device with their associated Hamiltonian H and overlap T blocks (see text). The dimers are symbolically represented by thick arrows and the impurity by a white dot. (b) Band structure along the Γ-J' direction; dashed line represents the surface states. (c) The thin and thick lines represent the transmission of the undoped and doped systems, respectively. The red (blue) correspond to P (B) doping, respectively.

The computational scheme, limited to the linear response, is similar to standard tight-binding implementations of transport [39] but with submatrices replacing the scalar on-site and hopping terms [38].

The system is represented by 8 unit cells of the Si(001)-$p(2 \times 2)$ surface repeated along the dimer chains direction. Such a supercell is repeated periodically in the two surface directions. In the direction perpendicular to the surface, ten Si layers are used and the bottom surface is passivated by hydrogen. A single substitutional impurity is introduced at the center of the dimer chain in each 352-atoms supercell and the atomic positions are fully relaxed. The ''on-site'' Hamiltonian H_L and hopping T_{LL} matrices associated with the two leftmost sections [see Fig. 3(a)] are used to build the infinite left electrode (idem for the right electrode) while the 5 central cells constitute the ''device'' characterized by its Hamiltonian matrix H_D. The device interacts with the left (right) electrode with the ''hopping block'' T_{LD} (T_{DR}).

The band structure along the $\Gamma J'$ direction of the undoped Si(100)-$p(2 \times 2)$ surface is represented in Fig. 3(b) where the upper (D_{up}) and lower (D_{down}) dimer atom surface bands have been highlighted. The transmission of the device is represented in Fig. 3(c). The thin lines repre-

sent the transmission of the undoped surface in the dimer chains direction. The structure in plateaus of integer conductance (in units of e^2/h) shows that our central device is large enough to recover the undoped surface properties on each of its sides. In particular, the two first plateaus around the gap represent the transmission associated with the occupied D_{up} and unoccupied D_{down} surface bands. The thick lines give the transmission upon doping by a single impurity at the surface.

Under B doping (P), the drop of conductance is significant below (above) the Fermi level, in particular, at energies corresponding to the occupied (empty) D_{up} (D_{down}) surface states. Clearly, a single B (P) impurity can significantly reduce the conductance associated with the occupied (unoccupied) surface conducting channel. The effect is dramatic for the D_{down} state as a single P impurity along the dimer chain can backscatter nearly all of the incoming wave packets. The situation is similar to what was observed in the case of doped CNTs where B impurities (P) were shown to strongly affect the conductance below (above) the Fermi level [38,40–42]. Therefore, even though in principle the surface states of unpassivated wires may contribute to the transport properties [13,17], it is important to realize that surface segregation of dopants will dramatically affect the transmission associated with these conduction channels.

In conclusion, we have shown that impurity surface segregation strongly affects the conductance associated with surface states in the case of unpassivated wires. Upon passivation, the large surface to bulk aspect ratio of SiNWs is expected to lead to the neutralization by surface defects of impurities up to a large critical concentration below which the conductivity will not raise rapidly with doping. The different behavior of P versus B doping with respect to segregation indicates that n-type or p-type doping may lead to significantly different conductance properties in wires as compared to bulk.

We are indebted to T. Albaret for LOTF [27] calculations. The authors acknowledge partial support from the French "ACI TransNanofils," région Rhône-Alpes, the French CNRS national supercomputing center (IDRIS, Orsay), and the CDCSP (Lyon I).

[1] Y. Wu *et al.*, Nano Lett. **4**, 433 (2004).
[2] M. Menon *et al.*, Phys. Rev. B **70**, 125313 (2004).
[3] Y. Cui *et al.*, Appl. Phys. Lett. **78**, 2214 (2001).
[4] Y. Cui, X. Duan, J. Hu, and C. M. Lieber, J. Phys. Chem. B **104**, 5213 (2000).
[5] Y. Cui and C. M. Lieber, Science **291**, 851 (2001).
[6] J.-Y. Yu, S.-W Chung, and J. R. Heath, J. Phys. Chem. B **104**, 11 864 (2000).
[7] Y. Cui *et al.*, Nano Lett. **3**, 149 (2003).
[8] D. D. D. Ma *et al.*, Science **299**, 1874 (2003).
[9] D. D. D. Ma, C. S. Lee, and S. T. Lee, Appl. Phys. Lett. **79**, 2468 (2001).
[10] K.-K. Lew *et al.*, Appl. Phys. Lett. **85**, 3101 (2004).
[11] S. Ismail-Beigi and T. Arias, Phys. Rev. B **57**, 11 923 (1998).
[12] Y. Zhao and B. I. Yakobson, Phys. Rev. Lett. **91**, 035501 (2003).
[13] R. Rurali and N. Lorente, Phys. Rev. Lett. **94**, 026805 (2005).
[14] R. Kagimura *et al.*, Phys. Rev. Lett. **95**, 115502 (2005).
[15] I. Ponomareva *et al.*, Phys. Rev. Lett. **95**, 265502 (2005).
[16] A. K. Singh *et al.*, Nano Lett. **5**, 2302 (2005).
[17] K. Kobayashi, Phys. Rev. B **69**, 115338 (2004).
[18] D. Xiangfeng *et al.*, Nature (London) **425**, 274 (2003).
[19] Z. Zhong *et al.*, Nano Lett. **5**, 1143 (2005).
[20] D. Pierreux and A. Stesmans, Phys. Rev. B **66**, 165320 (2002).
[21] Such surface defect concentrations have been recently measured for 10–15 nm diameter SiNWs. See A. Baumer *et al.*, Appl. Phys. Lett. **85**, 943 (2004).
[22] S. M. Sze, *Physics of Semiconductor Devices* (Wiley, New York, 1981).Note that in P:Si, $n_c(\mathrm{Mott}) = 3.7 \times 10^{18}\ \mathrm{cm}^{-3}$.
[23] J. Wang *et al.*, Appl. Phys. Lett. **86**, 093113 (2005).
[24] J. P. Perdew *et al.*, Phys. Rev. Lett. **77**, 3865 (1996).
[25] N. Troullier and J. L. Martins, Phys. Rev. B **43**, 1993 (1991).
[26] J. M. Soler *et al.*, J. Phys. Condens. Matter **14**, 2745 (2002).
[27] Six configurations of a $\langle 110 \rangle$ grown SiNW, with different surface reconstructions, were equilibrated in a series of molecular dynamics runs (time = 5 ps, $T = 1000$ K), using a tight-binding model for silicon within the learn on the fly (LOTF) method [28]. The lowest energy configuration was finally relaxed with the SIESTA code.
[28] G. Csanyi *et al.*, Phys. Rev. Lett. **93**, 175503 (2004).
[29] P. Bedrossian *et al.*, Phys. Rev. Lett. **63**, 1257 (1989).
[30] M. Ramamoorthy *et al.*, Phys. Rev. B **59**, 4813 (1999).
[31] All nonequivalent positions between bulk and surface, including subsurface sites, were tested.
[32] The band gap of SiNW-d (1.3 eV DFT value) is larger than that of bulk Si (0.55 eV DFT value) due to confinement effects. It is important, however, to recall that DFT significantly underestimates band gaps [33,34].
[33] Xinyuan Zhao *et al.*, Phys. Rev. Lett. **92**, 236805 (2004).
[34] Y.-M. Niquet *et al.*, Phys. Rev. B **73**, 165319 (2006).
[35] Similar results have been obtained for a P_{b1} defect at a model Si/SiO_2 interface. M. V. Fernández-Serra and X. Blase (to be published).
[36] This degenerate behavior is related to the rather large B concentration due to our supercell size.
[37] C.-C. Fu, M. Weissmann, and A. Saul, Surf. Sci. **494**, 119 (2001).
[38] Ch. Adessi, S. Roche, and X. Blase, Phys. Rev. B **73**, 125414 (2006).
[39] S. Datta, *Electronic Transport in Mesoscopic Systems* (Cambridge University Press, Cambridge, England, 1995).
[40] H. J. Choi, J. Ihm, S. G. Louie, and M. L. Cohen, Phys. Rev. Lett. **84**, 2917 (2000).
[41] C.-C. Kaun *et al.*, Phys. Rev. B **65**, 205416 (2002).
[42] S. Latil, S. Roche, D. Mayou, and J.-C. Charlier, Phys. Rev. Lett. **92**, 256805 (2004).